AGU100 ADVANCING EARTH AND SPACE SCIENCE

Geophysical Research Letters

RESEARCH LETTER
10.1029/2018GL079177

Key Points:
- The level of active lava lakes is a key parameter in their study but surprisingly hard to measure
- Eredar is a new radar system for monitoring surface level of active lava lakes
- At Erebus volcano it collected the longest continuous time series of lake level to date

Correspondence to:
N. J. Peters,
njp39@cam.ac.uk

Citation:
Peters, N. J., Oppenheimer, C., Brennan, P., Lok, L. B., Ash, M., & Kyle, P. (2018). Radar altimetry as a robust tool for monitoring the active lava lake at Erebus volcano, Antarctica. *Geophysical Research Letters*, *45*, 8897–8904. https://doi.org/10.1029/2018GL079177

Received 12 JUN 2018
Accepted 24 JUL 2018
Accepted article online 3 AUG 2018
Published online 2 SEP 2018

Radar Altimetry as a Robust Tool for Monitoring the Active Lava Lake at Erebus Volcano, Antarctica

N. J. Peters[1], C. Oppenheimer[1], P. Brennan[2], L. B. Lok[2], M. Ash[3], and P. Kyle[4]

[1]Department of Geography, University of Cambridge, Cambridge, UK, [2]Department of Electronic and Electrical Engineering, University College London, London, UK, [3]PA Consulting Group, Global Innovation and Technology Centre, Melbourn, UK, [4]Department of Earth and Environmental Sciences, New Mexico Institute of Mining and Technology, Socorro, NM, USA

Abstract The level of lava within a volcanic conduit reflects the overpressure within a connected magma reservoir. Continuous monitoring of lava level can therefore provide critical insights into volcanic processes and aid hazard assessment. However, accurate measurements of lava level are not easy to make, partly owing to the often dense fumes that hinder optical techniques. Here we present the first radar instrument designed for the purpose of monitoring lava level and report on its successful operation at Erebus volcano, Antarctica. We describe the hardware and data-processing steps followed to extract a time series of lava lake level, demonstrating that we can readily resolve ~1 m cyclic variations in lake level that have previously been recognized at Erebus volcano. The performance of the radar (continuous, automated data collection in temperatures of around −30 °C) indicates the suitability of this approach for sustained automated measurements at Erebus and other volcanoes with lava lakes.

Plain Language Summary Active lava lakes are the exposed top of a volcano's magmatic plumbing system. Although only found at a handful of volcanoes worldwide, they are important because they allow direct measurements of magmatic processes which at other volcanoes occur underground and out of sight. The surface level of these lakes is an important parameter to monitor, because it reflects pressure changes in the underlying magmatic system. However, it is remarkably difficult to measure, because their surface is often obscured by the volcanic gases emanating from the lava. We have developed the first radar instrument for monitoring lava lake level, which can effectively *see through* the volcanic gases, providing an accurate measure of lake level regardless of visibility. The radar was deployed at Erebus volcano, Antarctica and successfully recorded the longest-duration measurements of its lava lake's surface level made to date. The radar was able to clearly resolve the meter-scale variations in lake level that have previously been documented at Erebus. Our study shows that radar is a promising solution for long-duration studies of lava lakes, and we are working on refining our design into an operational tool to support volcanological studies and hazard assessment at other volcanoes around the world.

1. Introduction

Open-vent volcanoes maintain magma at or close to the surface, with persistent outputs of heat and gases (Rose et al., 2013). At the majority of these volcanoes, the interface between the magma and the atmosphere is obscured or only intermittently exposed within a narrow vent. However, a handful of open-vent volcanoes expose magma in plain view from the crater rim, in the form of an active lava lake which may persist for many decades (Tazieff, 1994). Examples are found at Nyiragongo (D.R. Congo), Erebus (Antarctica), and Erta 'Ale (Ethiopia). Such volcanoes are of particular importance to volcanology, as they allow direct observations to be made of magmatic processes that are normally hidden from view. Studies of active lava lakes have revealed many aspects of magma storage, transport, degassing, and eruption, highlighting also processes occurring within magma storage zones, conduit, and the lake itself (Patrick et al., 2016).

A key parameter in studying lava lakes is their surface level. This is indicative of pressure variations in the underlying magmatic system (Patrick et al., 2014) and also fluctuates (typically on shorter time scales) in response to shallower processes such as gas accumulation/release from the lake (Orr & Rea, 2012) and flow dynamics in the conduit (Jones et al., 2015; Peters, Oppenheimer, Killingsworth, et al., 2014).

Perhaps somewhat surprisingly, the surface level of active lava lakes is remarkably difficult to measure, especially over the extended time periods required for understanding their behavior and for operational monitoring. Previous studies (e.g., Patrick et al., 2014) have used thermal camera images, identifying the position of the surface against the back wall of the lake basin (either manually or using an automated approach) to estimate the surface height. However, the high temperature maintained by the encompassing basin following a rapid draining of the lake makes the margin difficult to identify for an automated system, and manual identification is extremely time consuming. Furthermore, this approach is affected by changes in the basin geometry and cannot detect level changes due to uplift or subsidence of the crater itself. It should also be noted that even at thermal infrared wavelengths, visibility of the lake can be, and particularly at Erebus often is, severely impacted by the volcanic plume. Plume opacity also impedes the use of stereo-imaging systems (Smets et al., 2017) and terrestrial laser scanning (TLS) technologies. TLS is a widely used tool in geoscience (Telling et al., 2017), and although some lava lake studies have been conducted using such devices (e.g., Jones et al., 2015), they are limited to rare time periods of exceptional visibility. TLS instruments are also expensive and delicate, making them unsuitable for long-duration deployment at volcanic craters.

Here we demonstrate that radar is an effective solution to lava lake level monitoring. Using a low-cost (~£3,000), custom-built radar system, named Eredar, we were able to obtain the longest continuous measurements of lake level at Erebus volcano to date, easily resolving the ~1 m variations in level that are typical of its behavior (Jones et al., 2015; Peters, Oppenheimer, Killingsworth, et al., 2014).

The aims of this article are twofold: (i) To present the design of our radar system and our data-processing strategy, which we believe will be of use to researchers undertaking radar system development in other fields, not just volcanology. (ii) To demonstrate the potential of radar for continuous and extended (operational) lava lake surveillance.

2. Erebus Volcano

Situated on Ross Island, Antarctica, Erebus is a 3,794-m-high active stratovolcano (Figure 1a). It is the world's most southerly active volcano and hosts the only known example of a phonolitic active lava lake (Figure 1b; Kelly et al., 2008). The lake at Erebus has been in place since at least 1972 (Giggenbach et al., 1973) and is characterized by stable convective behavior punctuated sporadically by Strombolian-type explosions caused by gas slugs entering the lake. Some of these explosions are large enough to partially empty the lake, with ejected material occasionally being thrown clear of the crater (Dibble et al., 2008; Jones et al., 2008). During periods of quiescence the lake exhibits a remarkable pulsatory behavior (Oppenheimer et al., 2009), with its surface motion, surface level, gas composition, and gas flux all varying on a timescale of 10–15 mins (Peters, Oppenheimer, Killingsworth, et al., 2014). This behavior is thought to reflect the flow dynamics of magma in the conduit feeding the lake (Oppenheimer et al., 2009; Peters, Oppenheimer, Kyle, et al., 2014); however, a comprehensive explanation has proved elusive and provides, in part, the motivation for the development of the Eredar radar system.

The Erebus lava lake was the subject of a previous study using radar undertaken by Gerst et al. (2013). However, this study focused on analyzing the evolution of explosive events in the lake, using a Doppler radar system to measure the expansion rate of large bubbles at the surface. No attempt to monitor the surface level of the lake was made, and the radar system was not considered for long-term deployment.

3. Methods

3.1. Field Deployment

Fieldwork on Erebus is conducted during the Austral Summer, typically between late November and early January. The Eredar radar was deployed on Erebus as part of the Mount Erebus Volcano Observatory's (MEVO) 2016 field campaign. Its installation was hampered by bad weather, and it was not in place until the very end of the campaign, resulting in a relatively short data set being obtained.

After initial testing at our field camp at around 3,450-m elevation (Figure 1c), the radar was installed at the so-called "Shackleton's Cairn" site on the northern side of the main crater, alongside Mount Erebus Volcano Observatory's thermal camera (Figure 1d; Peters, Oppenheimer, & Kyle, 2014). The antennas were mounted on custom-built heavy duty tripods, which were securely anchored to the ground. A tent was erected nearby to house the data-acquisition laptop and to provide shelter for the operator during the setup process. Alignment

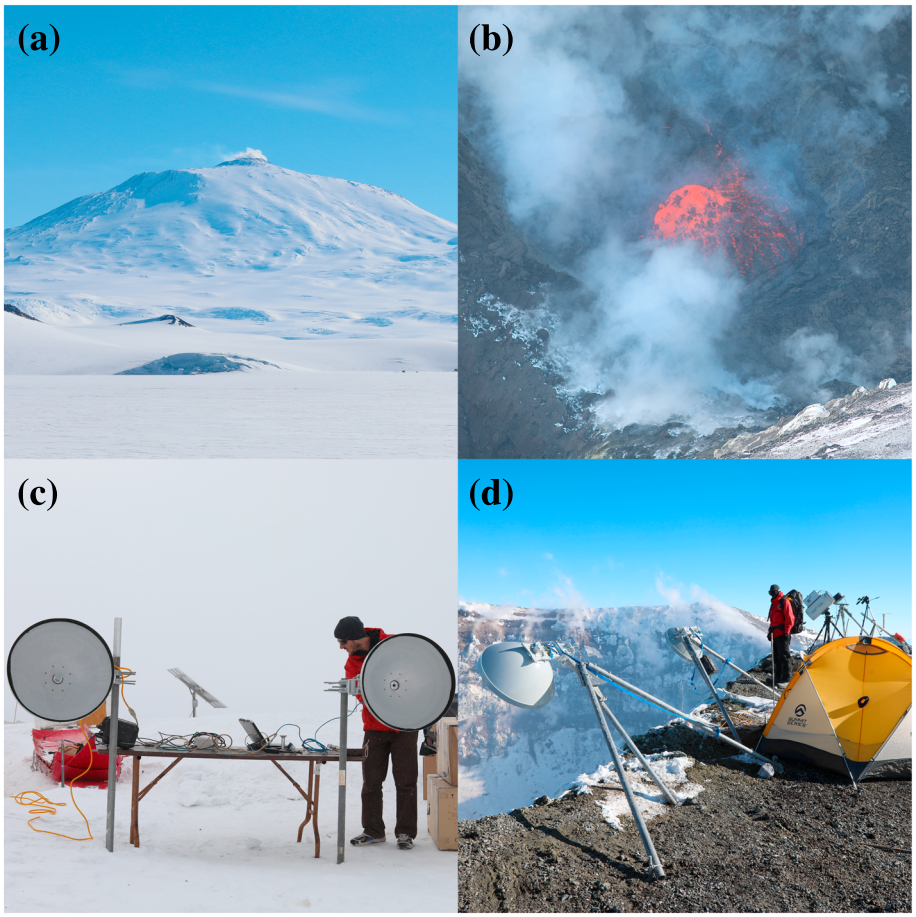

Figure 1. Field deployment of the Eredar radar in December 2016; (a) Erebus volcano, (b) its active lava lake as it appeared in 2016 (~30 m in diameter), (c) Eredar being tested at the field camp, (d) Eredar installed at the crater rim. The radar electronics are housed in the black case mounted on the far antenna tripod. The thermal camera and other monitoring instruments can be seen in the background.

of the antennas with the lava lake was achieved by placing an infrared thermometer into their waveguide feeds. The thermometer had approximately the same field of view (3°) as the antenna beam width (3.6°), and the antennas could then be pointed at the lake by adjusting them until a maximum temperature was recorded. The thermometer was removed prior to making radar measurements.

Following a supervised period of operation lasting ~6 hr on 15 December 2016, the radar was taken down again to avoid damage from an approaching storm. It was then redeployed on 19 December 2016 and ran, without user intervention, until it had to be shut down and removed at the end of the field season (21 hr later). The ambient temperature at the crater rim during this period was approximately −30 °C.

3.2. Radar Hardware

The Eredar instrument is a bespoke, frequency modulated continuous wave (FMCW) radar (e.g., Griffiths, 1990; Marshall & Koh, 2008) operating at X-band (10.2–10.6 GHz). Its design is loosely based on two previous geoscience radars constructed by researchers at University College London, namely, the Auto-pRES instrument (UHF, 300 MHz) used for ice shelf sounding (Lok et al., 2015) and the Geodar2 system (C-band, 5.3 GHz) used for avalanche monitoring (Ash et al., 2014). Due to the requirement of a narrow beam width for lava lake monitoring, the Eredar system operates at much higher frequency than these previous systems and therefore the details of its design are unique.

Figure 2 shows an overview of the Eredar design. An Analog Devices AD9914 direct digital synthesizer clocked at 3.5 GHz is used to produce a 900-1,300 MHz linear sweep in frequency. A band-pass filter is then used to select the first super-Nyquist image (e.g., Ash & Brennan, 2015) of this sweep at 2.6–2.2 GHz. The signal is amplified and split to provide the deramp signal for the receive chain and then up-converted using an 8-GHz

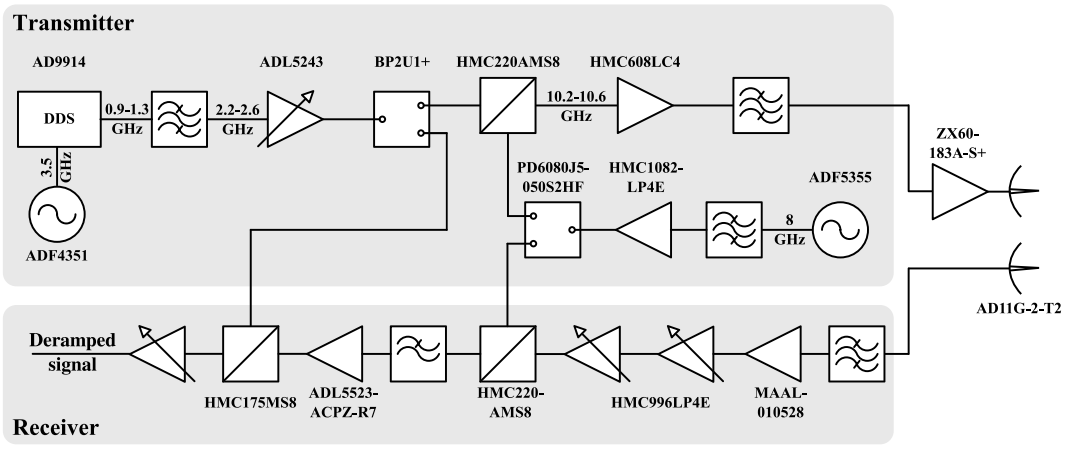

Figure 2. Simplified block diagram of the Eredar radar system. Some blocks represent an aggregation of several components and therefore do not have part numbers.

source produced by an Analog Devices ADF5355 synthesizer. A band-pass filter is used to remove unwanted mixing products resulting in a transmitted chirp (linear frequency sweep) of 10.6–10.2 GHz. A chirp duration of 0.16 s was used. To overcome higher than expected losses in our transmitter chain, we included an additional amplifier between the transmit output and the antenna. This brought our transmitted power up to ~15 dBm. On the receive side, the incoming signal is filtered and amplified using a chain of three low-noise amplifiers, before being down-converted using the 8-GHz signal and subsequently using the deramp signal from the transmitter. The deramped signal is then passed through an active filter stage which performs frequency gain control (Stove, 1992, 2004) to compensate for the drop in signal strength with range, thus maximizing the dynamic range available from the system's analog to digital converter (ADC). Additionally, the active filter suppresses signals above the Nyquist frequency of the ADC (>40 kHz) and also removes low-frequency signals caused by direct coupling between transmitter and receiver. The filtered, deramped signal is digitized using a 16-bit ADC clocked at 80 kHz. The ADC clock is precisely aligned with the control signal to the direct digital synthesizer used to initiate frequency ramping, ensuring interchirp coherence in a similar manner to Brennan et al. (2014). Eredar's onboard microprocessor is not sufficiently powerful to perform real-time processing on the digitized data. Instead, it is streamed over Ethernet and recorded on a laptop computer, with all processing being performed off-line at a later date. Ten chirps were averaged for each measurement, and measurements were made at a rate of ~0.25 Hz.

Both transmit and receive use 66-cm diameter Trango AD11G-2-T2 dish antennas, with a 3-dB beam width of 3.6° and a gain of 36 dBi. Given a range of 315 m and an incidence angle of 43° (typical viewing geometry of the lake at Erebus; Figure 1d), this gives a beam footprint approximately 27 m in diameter at the surface of the lake. This is comparable to the lake size itself, which typically varies between 30 and 50 m in diameter (Figure 1b).

The crater rim of Erebus is provided with 230-V AC power from a nearby solar and wind generation site (see Peters, Oppenheimer, and Kyle, 2014, for details). Due to its requirement of both positive and negative voltage supplies, the radar uses a center-tapped transformer and diode network to step down and rectify the main supply producing +7 VDC and −7 VDC. These supplies are then fed into a bank of linear regulators to produce the various supply rails required. Switching power supplies were deliberately avoided to keep noise on the power rails to a minimum. Total power consumption is in the order of 21 W, although around 50% of this is dissipated as heat in the linear regulators.

The 10.2- to 10.6-GHz frequency range was selected as a compromise between the cost of components and the requirement of a narrow beam width. For a given antenna size, beam width scales inversely with frequency. However, above 11 GHz there are very few mass-produced components available, resulting in a considerable increase in price.

The range resolution of an FMCW radar is given by $\frac{c}{2B}$, where c is the propagation velocity and B is the band width. High band width radars are more challenging and costly to construct due to the diminished gap between in-band signals and unwanted spurs and the difficulty in wideband matching of components.

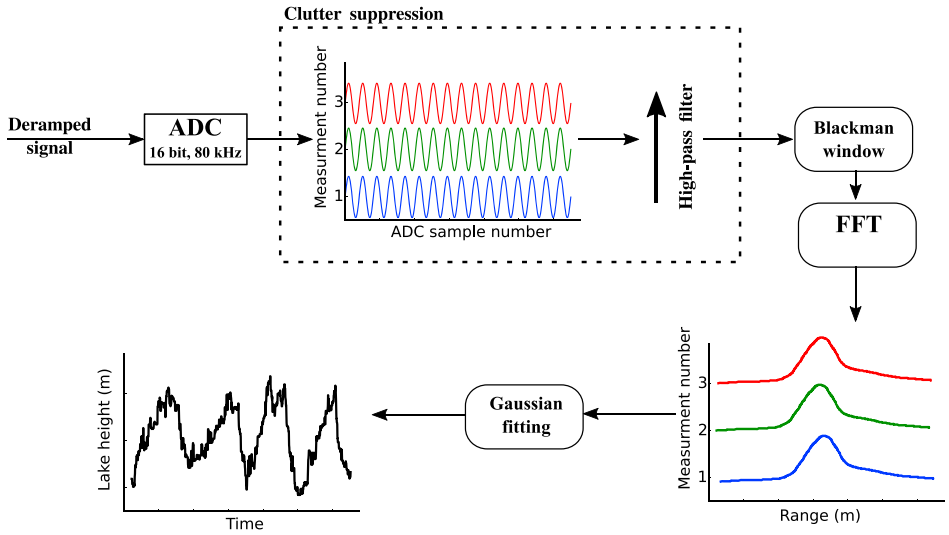

Figure 3. Block diagram showing the data-processing steps required to go from raw receiver output to lake level measurements. Each chirp is digitized and recorded. The digitized data are then high-pass filtered across all measurements to remove static clutter. Filtered data are then Blackman windowed and Fourier transformed to convert to range. The lake is identified in the range data by fitting a Gaussian to it. The mean of this Gaussian is used as the slant range to the lake. Finally, the slant ranges may be easily converted to lake level by considering the viewing geometry.

In addition, for a distributed target (such as lava lake surface), which will anyway span many range bins, there is little need for excessive range resolution since resolving individual reflectors on the lake's surface is not required. The Eredar system uses a band width of 400 MHz giving a range resolution of 37.5 cm. This was chosen as a reasonable compromise between range resolution and ease and cost of design.

The temporal resolution of an FMCW radar is determined fundamentally by the chirp period used, which in turn is determined by the maximum range required. In the case of the Eredar system, however, the temporal resolution was limited by the data throughput rate of the microcontroller rather than the chirp period. This limitation was unexpected and will be addressed in future versions of the radar through the use of higher speed data buses and better optimized software.

3.3. Data Processing

The data-processing steps required to obtain a lake level measurement from the receiver output are shown in Figure 3. The data are first conditioned using a clutter suppression algorithm (described below) to remove stationary targets. They are then windowed using a Blackman window and Fourier transformed using an fast Fourier transform (FFT) algorithm. The Blackman window is used to remove edge discontinuities that would otherwise be caused by the implicit rectangular window imposed by the finite duration of sampling. The windowed data are zero padded up to a length of 2^{16} prior to applying the FFT. Range is obtained from the frequency (post-FFT) data using the standard FMCW range equation (e.g., Griffiths, 1990) $r = f \cdot \frac{c\tau}{2B}$, where r is range, f is frequency, c is the propagation velocity, τ is the chirp period, and B is the chirp bandwidth. This assumes that objects are not moving during the chirp period, a reasonable assumption at Erebus where typical lake surface velocities are in the order of centimeters per second (Peters, Oppenheimer, Kyle, et al., 2014). The lake level is extracted from the range data by applying a Gaussian fit to it, as described below.

3.3.1. Clutter Suppression

Clutter (unwanted targets within a radar's field of view) is a common problem for surface-viewing radars, and many approaches have been developed to suppress it (e.g., Ash et al., 2018; Hyun et al., 2016; Martone et al., 2014). The crater in which the Erebus lava lake resides is littered with lava bombs and angular rocks from the crater walls. These have a much larger radar cross section compared to the relatively flat surface of the lava lake and produce strong reflections even when not at boresight. The clutter signal was found to be so great that the much weaker lake signal was entirely masked. A common approach to recovering a moving target signal from a stationary-clutter-dominated measurement is to high-pass filter the range-time data to remove stationary targets. Although this approach was found to work well when recovering point targets (e.g., a person walking in the radar beam) during testing, it did not work with data collected of the lake. This was partly due to the

low velocity of the lake surface parallel to boresight (on the order of 1×10^{-3} m/s) and partly due to the lake being a distributed target. The radar's oblique view of the lake means that its surface occupies many range bins in the recorded data. A change in surface level of the lake manifests itself as a rather subtle change in the distribution of amplitudes across these range bins, and as such is severely muted by high-pass filtering. Instead, we adopted a similar approach to Ash et al. (2018), performing clutter suppression on the raw radar data prior to conversion to range. Chirps from a measurement period are stacked coherently in time, and then high-pass filtered before being Fourier transformed and converted to range. Such an approach is made possible by the high degree of coherence between chirps of the Eredar system. We used an infinite impulse response (IIR) high-pass elliptic filter with an order of 10 and a cutoff frequency of 3×10^{-2} Hz. Due to the small size of the Erebus lake (relative to the antenna beam width), returns due to antenna sidelobes will be from stationary objects outside of the lake's surface and therefore will be effectively removed by the clutter suppression.

3.3.2. Lake Level Calculation

As noted above, the lake surface spans many range bins and as such manifests itself as a broad, smeared-out return rather than a sharp peak in range. Condensing this into a single value for lake slant range is somewhat subjective. We trialed three different approaches to extracting lake level from the radar return data; using the range bin with the maximum return power, using the lowest-range bin above a certain return power threshold (i.e., the first return from the lake's surface) and fitting a Gaussian function to the data and using its mean as the slant range to the lake. The logic of the latter approach is that to a good approximation, the antenna radiation pattern can be modeled as a Gaussian. If one assumes an approximately uniform cross section for all parts of the lake surface, the shape of the range profile is dominated by the radiation pattern of the antennas (note that the drop in return power due to increasing range is already accounted for by the active filter stage in the radar hardware).

A distributed target (such as the lake's surface) may be thought of as a large collection of point scatterers. The received signal at the radar is the sum of the contributions from all the scatterers. Since the lake surface is in constant motion, the phases of these contributions will be constantly changing, causing differences in return power for different ranges as the scattering contributions combine in phase or antiphase. Furthermore, visual inspection of the Erebus lake surface shows that it is far from being a uniform collection of scatterers. Numerous cracks in the lake's semisolid crust exist at any given instant and these also move with time.

Since both the maximum return power and the first return method for identifying the lake range are based on a single range bin, they are particularly susceptible to the effects detailed above. It should not be surprising therefore, that although all three techniques give a similar result when time-averaged, the scatter in range is much smaller ($\sim \pm 0.5$ m) for the Gaussian fit method than for the other methods, which have a scatter of approximately ± 2 m. For this reason, we found the Gaussian fit method the most satisfactory for the data presented in this manuscript.

The slant range to the lake was converted to a relative lake level using the following equation $L = (\bar{r} - r)\sin\theta$, where L is relative lake level, $\bar{r}$ is mean slant range (determined from the full time series of measurements), r is slant range, and θ is the grazing angle of the radar beam on the lake surface (measured as 42° using an inclinometer). Thus, a low stand of the lake (resulting in a higher than average slant range) gives a negative value of relative lake level.

4. Results and Discussion

Figure 4 shows a representative 2-hr window of the data recorded on 19 December 2016. The dominance of static clutter is very evident in the unprocessed data, and it is somewhat remarkable that a relatively simple clutter suppression algorithm is so successful at removing it and revealing the variations in lake height so clearly. Lake level is plotted as a relative height about its mean value, showing variations on the order of ± 0.5 m. This is consistent with the lake level changes measured by Jones et al. (2015) using TLS in 2010. The fluctuations in lake level shown in Figure 4 exhibit a cyclic behavior with a period of ~15 min. This is a well-recognized behavior of the Erebus lake as noted by numerous previous studies (Ilanko et al., 2015; Oppenheimer et al., 2009; Peters, Oppenheimer, Killingsworth, et al., 2014, Peters, Oppenheimer, Kyle, et al., 2014).

The lake levels presented in Figure 4 show a random measurement to measurement deviation of ± 0.5 m. We attribute this scatter to uncertainties in the Gaussian fitting and the rapidly changing specular nature of

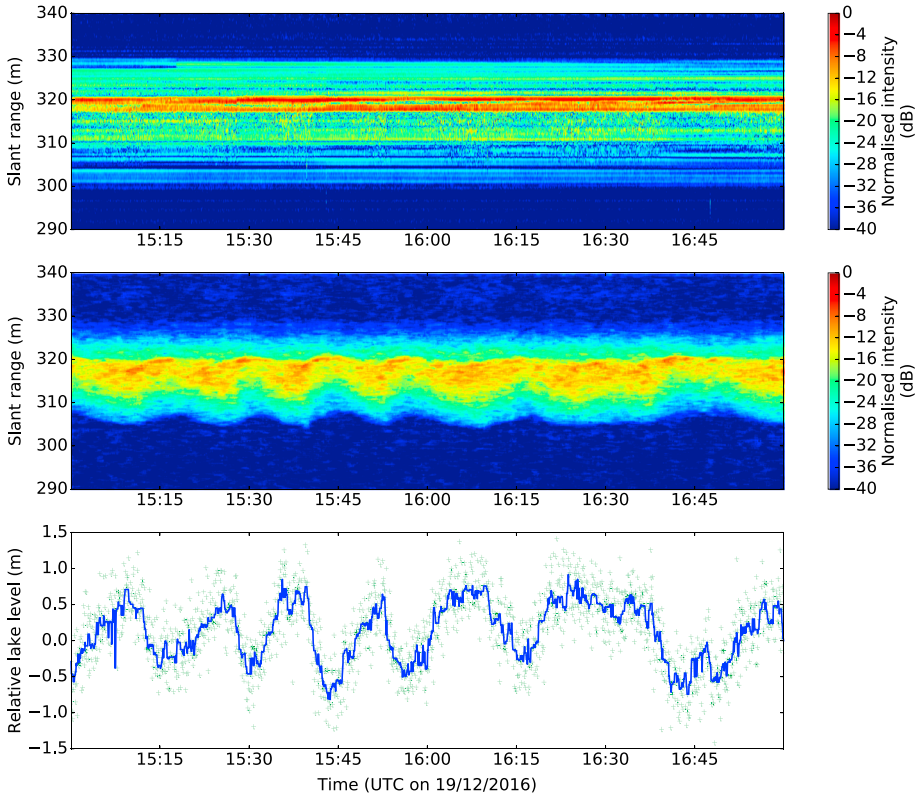

Figure 4. Representative 2-hr period of radar data acquired on 19 December 2016 showing raw slant range data (top), slant range data following clutter suppression (middle), and lake level relative to its mean (bottom). Green crosses show the lake level measurements, and the blue line shows the median filtered data (kernel size of 13).

the lake surface itself. Some measurements (e.g., at 16:14:20 UTC) show deviations of a few meters from their neighboring measurements. These are caused by meter-scale bubbles bursting at the lake's surface, forming a strong radar target at a particular range and skewing the Gaussian fit toward that range. This is confirmed by inspection of coincident thermal imagery collected with an automated infrared camera system (Peters, Oppenheimer, & Kyle, 2014).

5. Conclusions

We have presented the Eredar instrument, a new FMCW radar system designed for monitoring the level of active lava lakes, which was successfully deployed on Erebus volcano, Antarctica in December 2016. The data set recorded during this deployment is the longest continuous measure of lake level at Erebus to date and clearly demonstrates the potential of radar instruments for prolonged and continuous surveillance of lava lake level.

Future refinement of the system will include reducing power consumption, increasing acquisition rate, and incorporating onboard data-processing capabilities. The envisaged endpoint is a system suitable for long-term operational monitoring in support of volcanological research and hazard assessment.

Acknowledgments
This work was supported by the Isaac Newton Trust project "Physical constraints for the interpretation of open-vent volcanism" and NERC [grant NE/N009312/1]. CO is additionally supported by the NERC Centre for the Observation and Modelling of Volcanoes, Earthquakes and Tectonics (COMET). Field support was provided by the NSF under award ANT1142083. NP wishes to thank Aaron Curtis and Tim & Zoe Burton for their help during fieldwork. The radar data presented in this article may be obtained from https://doi.org/10.6084/m9.figshare.6480275.v1.

References

Ash, M., & Brennan, P. V. (2015). Transmitter noise considerations in super-Nyquist FMCW radar design. *Electronics Letters*, *51*(5), 413–415. https://doi.org/10.1049/el.2014.4236

Ash, M., Ritchie, M., & Chetty, K. (2018). On the application of digital moving target indication techniques to short-range FMCW radar data. *IEEE Sensors Journal*, *18*(10), 4167–4175. https://doi.org/10.1109/JSEN.2018.2823588

Ash, M., Tanha, M. A., Brennan, P. V., Köhler, A., McElwaine, J. N., & Keylock, C. J. (2014). Improving the sensitivity and phased array response of FMCW radar for imaging avalanches. In *2014 International Radar Conference*, pp. 1–5. https://doi.org/10.1109/RADAR.2014.7060387

Brennan, P. V., Lok, L. B., Nicholls, K., & Corr, H. (2014). Phase-sensitive FMCW radar system for high-precision Antarctic ice shelf profile monitoring. *IET Radar, Sonar & Navigation*, *8*(7), 776–786. https://doi.org/10.1049/iet-rsn.2013.0053

Dibble, R., Kyle, P., & Rowe, C. (2008). Video and seismic observations of Strombolian eruptions at Erebus volcano, Antarctica. *Journal of Volcanology and Geothermal Research*, *177*(3), 619–634. https://doi.org/10.1016/j.jvolgeores.2008.07.020

Gerst, A., Hort, M., Aster, R. C., Johnson, J. B., & Kyle, P. R. (2013). The first second of volcanic eruptions from the Erebus volcano lava lake, Antarctica—Energies, pressures, seismology, and infrasound. *Journal of Geophysical Research: Solid Earth*, *118*, 3318–3340. https://doi.org/10.1002/jgrb.50234

Giggenbach, W. F., Kyle, P. R., & Lyon, G. L. (1973). Present volcanic activity on Mount Erebus, Ross Island, Antarctica. *Geology*, *1*(3), 135–136.

Griffiths, H. D. (1990). New ideas in FM radar. *Electronics Communication Engineering Journal*, *2*(5), 185–194. https://doi.org/10.1049/ecej:19900043

Hyun, E., Jin, Y.-S., & Lee, J.-H. (2016). A pedestrian detection scheme using a coherent phase difference method based on 2D range-Doppler FMCW radar. *Sensors*, *16*(1), E124. https://doi.org/10.3390/s16010124

Ilanko, T., Oppenheimer, C., Burgisser, A., & Kyle, P. (2015). Cyclic degassing of Erebus volcano, Antarctica. *Bulletin of Volcanology*, *77*(6), 56. https://doi.org/10.1007/s00445-015-0941-z

Jones, K. R., Johnson, J. B., Aster, R., Kyle, P. R., & McIntosh, W. (2008). Infrasonic tracking of large bubble bursts and ash venting at Erebus volcano, Antarctica. *Journal of Volcanology and Geothermal Research*, *177*(3), 661–672. https://doi.org/10.1016/j.jvolgeores.2008.02.001

Jones, L. K., Kyle, P. R., Oppenheimer, C., Frechette, J. D., & Okal, M. H. (2015). Terrestrial laser scanning observations of geomorphic changes and varying lava lake levels at Erebus volcano, Antarctica. *Journal of Volcanology and Geothermal Research*, *295*, 43–54. https://doi.org/10.1016/j.jvolgeores.2015.02.011

Kelly, P. J., Kyle, P. R., Dunbar, N. W., & Sims, K. W. (2008). Geochemistry and mineralogy of the phonolite lava lake, Erebus volcano, Antarctica: 1972–2004 and comparison with older lavas. *Journal of Volcanology and Geothermal Research*, *177*(3), 589–605. https://doi.org/10.1016/j.jvolgeores.2007.11.025

Lok, L. B., Brennan, P. V., Ash, M., & Nicholls, K. W. (2015). Autonomous phase-sensitive radio echo sounder for monitoring and imaging Antarctic ice shelves. In *2015 8th International Workshop on Advanced Ground Penetrating Radar (IWAGPR)*, pp. 1–4. https://doi.org/10.1109/IWAGPR.2015.7292636

Marshall, H.-P., & Koh, G. (2008). FMCW radars for snow research. *Cold Regions Science and Technology*, *52*(2), 118–131. https://doi.org/10.1016/j.coldregions.2007.04.008

Martone, A. F., Ranney, K., & Le, C. (2014). Noncoherent approach for through-the-wall moving target indication. *IEEE Transactions on Aerospace and Electronic Systems*, *50*(1), 193–206. https://doi.org/10.1109/TAES.2013.120329

Oppenheimer, C., Lomakina, A. S., Kyle, P. R., Kingsbury, N. G., & Boichu, M. (2009). Pulsatory magma supply to a phonolite lava lake. *Earth and Planetary Science Letters*, *284*(3-4), 392–398. https://doi.org/10.1016/j.epsl.2009.04.043

Orr, T. R., & Rea, J. C. (2012). Time-lapse camera observations of gas piston activity at Pu'u 'Ō'ō, Kīlauea volcano, Hawai'i. *Bulletin of Volcanology*, *74*(10), 2353–2362. https://doi.org/10.1007/s00445-012-0667-0

Patrick, M. R., Orr, T., Antolik, L., Lee, L., & Kamibayashi, K. (2014). Continuous monitoring of Hawaiian volcanoes with thermal cameras. *Journal of Applied Volcanology*, *3*(1), 1. https://doi.org/10.1186/2191-5040-3-1

Patrick, M. R., Orr, T., Swanson, D. A., & Lev, E. (2016). Shallow and deep controls on lava lake surface motion at Kīlauea Volcano. *Journal of Volcanology and Geothermal Research*, *328*, 247–261. https://doi.org/10.1016/j.jvolgeores.2016.11.010

Peters, N., Oppenheimer, C., Killingsworth, D. R., Frechette, J., & Kyle, P. (2014). Correlation of cycles in lava lake motion and degassing at Erebus volcano, Antarctica. *Geochemistry, Geophysics, Geosystems*, *15*, 3244–3257. https://doi.org/10.1002/2014GC005399

Peters, N., Oppenheimer, C., & Kyle, P. (2014). Autonomous thermal camera system for monitoring the active lava lake at Erebus volcano, Antarctica. *Geoscientific Instrumentation, Methods and Data Systems*, *3*(1), 13–20. https://doi.org/10.5194/gi-3-13-2014

Peters, N., Oppenheimer, C., Kyle, P., & Kingsbury, N. (2014). Decadal persistence of cycles in lava lake motion at Erebus volcano, Antarctica. *Earth and Planetary Science Letters*, *395*, 1–12. https://doi.org/10.1016/j.epsl.2014.03.032

Rose, W. I., Palma, J. L., Granados, H. D., & Varley, N. (2013). Understanding open-vent volcanism and related hazards. Geological Society of America.

Smets, B., d'Oreye, N., Kervyn, M., & Kervyn, F. (2017). Gas piston activity of the Nyiragongo lava lake: First insights from a stereographic time-lapse camera system. *Journal of African Earth Sciences*, *134*, 874–887. https://doi.org/10.1016/j.jafrearsci.2016.04.010

Stove, A. G. (1992). Linear FMCW radar techniques. *IEE Proceedings F - Radar and Signal Processing*, *139*(5), 343–350. https://doi.org/10.1049/ip-f-2.1992.0048.

Stove, A. G. (2004). Modern FMCW radar—Techniques and applications. In *First European Radar Conference, 2004. EURAD.*, pp. 149–152.

Tazieff, H. (1994). Permanent lava lakes: Observed facts and induced mechanisms. *Journal of Volcanology and Geothermal Research*, *63*(1–2), 3–11. https://doi.org/10.1016/0377-0273(94)90015-9

Telling, J., Lyda, A., Hartzell, P., & Glennie, C. (2017). Review of Earth science research using terrestrial laser scanning. *Earth-Science Reviews*, *169*, 35–68. https://doi.org/10.1016/j.earscirev.2017.04.007